Towards Efficient Wireless Power Transmission for Implantable Devices Using Three-Coil Receivers and Metamaterial Lenses

Journal:	*Transactions on Microwave Theory and Techniques*
Manuscript ID	TMTT-2022-09-1401
Manuscript Type:	Original Manuscript
Date Submitted by the Author:	27-Sep-2022
Complete List of Authors:	Wong, Blake; University of Hawai'i at Manoa Iskander, Magdy; University of Hawai'i at Manoa Yun, Zhengqing; University of Hawai'i at Manoa Xiao, Yuanzhang; University of Hawai'i at Manoa Clemens, Scott; University of Hawai'i at Manoa
Keywords:	metamaterial lens, multi-layered tissue model, non-radiative inductive coupling, three orthogonal coils, HFSS

Towards Efficient Wireless Power Transmission for Implantable Devices Using Three-Coil Receivers and Metamaterial Lenses

Blake Wong, *Student Member, IEEE,* Magdy F. Iskander, *Fellow, IEEE,* Zhengqing Yun, *Senior Member, IEEE,* Yuanzhang Xiao, *Member, IEEE,* and Scott Clemens

***Abstract*— Efficient wireless power transfer (WPT) is crucial because it reduces the charging time of the implantable device and potentially minimizes heating effects that can severely damage the patient's tissue. This paper explores two methods to increase WPT efficiency: introducing a new WPT system using three orthogonal receiving coils and, secondly, including a metamaterial lens in a WPT system. Simulations in this study were conducted using a 3D, realistic multi-layer cross-section of the human body, reported complex permittivity properties as a function of frequency, and High Frequency Structure Simulator (HFSS) used to calculate transmission and reflection coefficient parameters. The simulation results using the three orthogonal receiving coils show that the new system not only mitigated the reduction in power transfer efficiency due to implantable rotation, but it contributed to improved power transfer efficiency under the effects of rotation within the human body. Also, the simulation results of a metamaterial lens redesigned to suit lower frequencies showed an increase in power transmission efficiency of 3.2 dB to 7.6 dB at a frequency range between 100 kHz to 5 MHz. The optimal distance for the metamaterial lenses from the human body is also examined. It is shown that it is necessary to maintain a distance of 0.5 to 2 cm between the metamaterial lens and the human body to help prevent detuning the lens efficiency.**

***Index Terms*—HFSS, metamaterial lens, multi-layered tissue model, non-radiative inductive coupling, three orthogonal coils**

I. Introduction

Large separation distances between transmitting (Tx) and receiving (Rx) coils, angular and transpositional misalignment between coils, and tissue losses limit the power transmission performance in Non-Radiative Inductive Coupling (NRIC) wireless power transmission (WPT) systems [1].

Some earlier works have simulated and experimentally tested in free space that omnidirectional receiver coils successfully helped mitigate the sharp decreases of transmitted power from the self-rotational effects of the implantable device [2],[3]. However, these papers did not discuss the effectiveness of the three orthogonal receiver coils, typically housed in a titanium shell needed to protect the surrounding tissue. Also, none of these papers investigated any effects of power transmission in practical applications where the implantable unit with the three orthogonal coils are placed in a multi-layer tissue human body model. Lastly, the 3D circular coil design in these papers does not share the same shape as the rectangular titanium implantable units found in commercially available products.

The first part of this paper addresses the effectiveness of using three orthogonal coils in an effective and realistically modeled wireless transmission arrangement for charging implantable devices. We propose to add more receiving coils in the implantable unit to collect more power and improve the power transfer efficiency. A 3D design with orthogonal coils used in Wireless Capsule Endoscopy (WCE) power transmission is adopted for the receiving coils. They are positioned around a central axis, maximizing the power transmission under rotation effects. When the three orthogonal coils are not perfectly in line with the transmitter coil field lines, the field lines missed by one coil are received by the other two coils [4]. Like NRIC, WCE implantable devices face challenges in power efficiency due to the significant separation distances between the Tx and Rx coils, unpredictability in capsule orientation and motion, and the need for a compact size of the receiving coil [5]. Our wireless power transmission 3D receiving coil design simulated in High Frequency Structure Simulator (HFSS) software maximizes the space of the rectangular implantable unit resulting in a maximized effective area of each of the three coils. These characteristics in our design show increased power received while minimizing interferences among the receiving coils.

Various metamaterial lenses in free space placed between the Tx and Rx coils to help focus the magnetic field in the direction of the Rx coil's location has been proposed and tested in several earlier publications [6]-[8]. These metamaterials were tuned, achieving resonance in the high kHz to low MHz frequency range. In [6], changing the capacitance value of the four adjustable capacitors connected to four coils allowed

This work was supported in part by the U.S. National Science Foundation under Grant 1822213.

The authors are with Hawaii Advanced Wireless Technologies Institute at the University of Hawaii, Manoa, Honolulu, HI, USA (correspondence e-mail: magdy.iskander@gmail.com).

reconfigurability of the metamaterial lens for a selected frequency. However, the metamaterial's design was optimized for a frequency range between 14.1 MHz and 25 MHz which is outside the frequency ranges found in commercially available WPT systems. Other WPT systems, including a superlens metamaterial design found in [7], effectively concentrated the magnetic fields of the source but were too bulky to be applied in realistic applications. A metamaterial lens presented in [8], proposed an optimal design in the kHz frequency range for wireless charging in drone applications. Unfortunately, the results were measured in free space applications and did not discuss the multi-layer tissue interactions and potential power losses associated with the metamaterial lens at different distances from the skin's surface.

We also explored the implementation of a metamaterial lens to improve power transfer efficiency between receiver and transmitter coils. The procedure starts by simulating and calculating the power transmission efficiency with and without a resonant metamaterial focusing board. We then conducted a parametric study to determine the optimal location of the metamaterial board between the transmitter and the human body. Next, we examined the power transmission efficiency with and without the metamaterial board at different frequencies. To incorporate the metamaterial lens in pre-existing commercially available WPT systems, we tuned our metamaterial lens to target lower frequency ranges. By lowering the frequency, we increased the number of turns for each coil on the metamaterial surface.

In Section II, we describe the system design of the 3D receiving orthogonal coils in part A, and the redesigned metamaterial lens in part B. Section III includes the simulation results for the 3D Receiving orthogonal coil design in part A and the redesigned metamaterial lens in part B. Section IV summarizes our results and includes our future work.

II. System Design

A. 3D Receiving Orthogonal Coils

The 3D rectangular orthogonal receiver (Rx) coils' dimensions begin with the largest coil facing the transmitting coil, represented as coil #1, l_{rx1} = 4 cm, w_{rx1} = 2.5 cm, d_{rx1}= 0.6 cm. The intermediate coil faced horizontally represents coil #2 is l_{rx2} = 3.9 cm, w_{rx2} = 0.85 cm. The innermost coil faced vertically represents coil #3 is l_{rx3} = 2.4 cm, w_{rx3} = 0.7 cm. The number of turns for each of the 3 receiving coils beginning with coil 1 set at 10 turns while coils 2 and 3 have a single turn. The cross-sectional area of the copper wire is 0.1mm^2. In Fig. 1, we do not expect coils 2 and 3 to receive the same power as coil 1. However, we expect incremental increases proportional to each coil's relative areas and the number of turns.

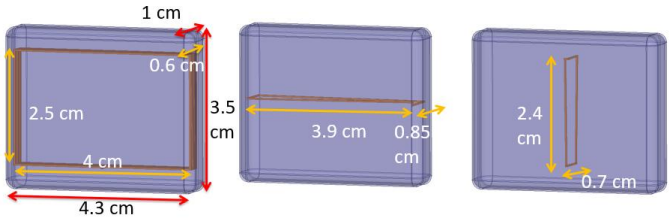

Fig. 1. (a) Coil 1 (facing the transmitter coil) 10 cm^2, (b) Coil 2 (horizontally faced) 3.31 cm^2, (c) Coil 3 (vertically faced) 1.68 cm^2.

The titanium case encapsulates the orthogonal Rx coils protecting the surrounding tissues. The dimensions of the titanium case are 4.3 x 3.5 x 1 (cm) with a shell thickness of 0.25 mm. The Rx coils are modelled inside a titanium case with a conductivity of 5.85×10^5 (S/m) placed within the abdominal fat layer of the human body model shown in Fig. 2.

The Tx coil will be located on the skin surface in front of the subcutaneous Rx coils to reduce the distance between the Tx and Rx. The single-turn circular planar Tx coil has a diameter D_{tx} = 5.28 cm. The transmitter coil is slightly larger than the receiving coils to tolerate misalignment conditions sufficiently.

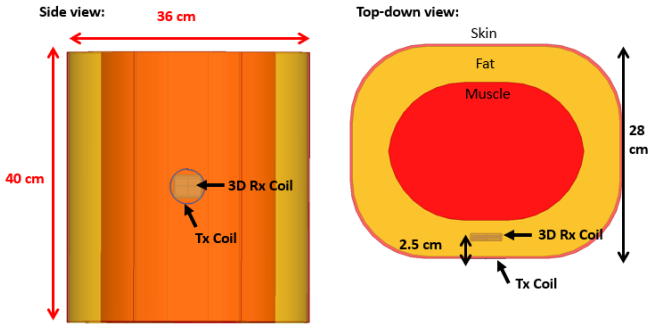

Fig. 2. Transmitter and 3D orthogonal receiver coils in the multi-layer tissue model: Side view (left) and Top-down view (right).

An adult male's torso comprises a multi-layer elliptical cylinder with a torso width of w_{torso} = 36 cm, depth of torso d_{torso} = 28 cm, and a torso height h_{torso} = 40 cm. The multi-layered cylinders consist of three different biological tissues: skin (external layer of thickness t_s = 0.3 cm), fat (intermediate layer of thickness t_f = 5 cm), and muscle (inner part). The dielectric properties at 40 kHz of the biological tissues are [9]:

Skin: ε_r = 1130, μ_r = 1, σ = 0.000249 (S/m);
Fat: ε_r = 197, μ_r = 1, σ = 0.0432 (S/m);
Muscle: ε_r = 11000, μ_r = 1, σ = 0.35 (S/m);

B. Metamaterial Lens

To further enhance the system's magnetic field and power transfer efficiency, we explored incorporating a metamaterial lens into a wireless power transmission system [6]. The metamaterial lens design shown in Fig. 3 comprises of 4-unit

cells with an FR4 substrate dimension of 22 cm x 22 cm x 0.12 cm. The coil dimensions are 9.6 cm x 9.2 cm, and the copper coils and contacts have a width of 0.2 cm and a thickness of 5 mils ~ 0.0127 cm. The metamaterial lens coil inductances are calculated using the impedance values in HFSS. Using the inductance value, we calculate the lumped capacitance for a given frequency using the resonance frequency equation defined by (1):

$$f = \frac{1}{2\pi\sqrt{LC}} \quad (1)$$

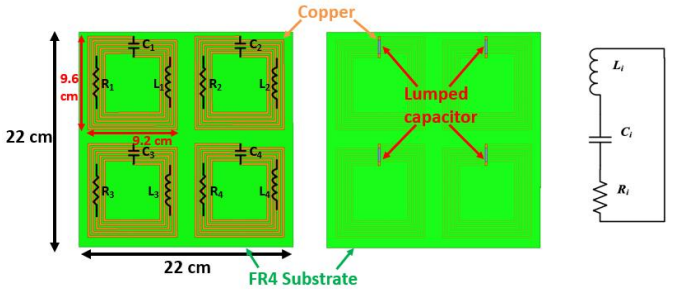

(a) (b) (c)

Fig. 3. Metamaterial lens: (a) Front (Facing Rx coil), (b) Back (Facing Tx coil), (c) Equivalent RLC resonant circuit of the unit cell coil structure [6].

The Tx and Rx FR4 substrate dimensions are identical, set at 11 cm x 11 cm, and the coil dimensions are 9.6 cm x 9.2 cm, as shown in Fig. 4.

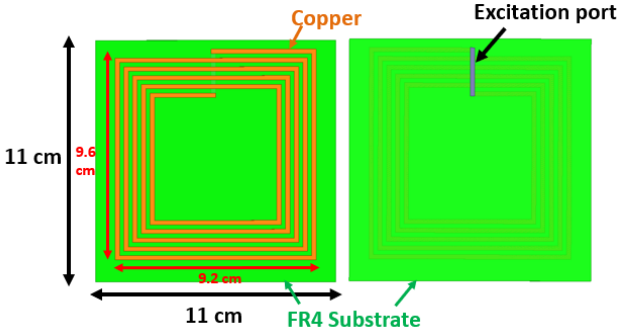

(a) (b)

Fig. 4. Tx coil and Rx coil: (a) Front side, (b) Back side of the substrate.

The separation distance between the Rx and Tx coils is 12 cm. The metamaterial surface is exactly in the middle of the Tx and Rx coils. There is a 1 cm gap between the metamaterial lens and the skin's surface of the multi-layered tissue model shown in Fig. 5.

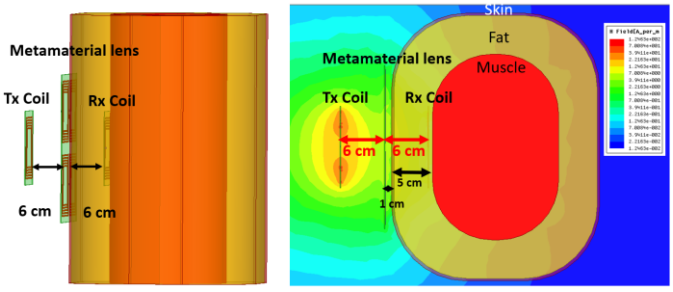

(a) (b)

Fig. 5. Metamaterial lens with Human Body model: (a) Side view, (b) Top view.

III. Simulation Results

A. 3D Receiving Orthogonal Coils

We examine the performance of the 3D orthogonal receiver coils for three rotations around the central coordinate axis. The power transmission for each coil is recorded, performing a plus/minus 60° rotation around each axis, with steps of 30° [10]. The total power is the sum of the powers received by each of the three Rx coils. The surface area of coil 1 is 10 cm^2; coil 2 is 3.31 cm^2, and coil 3 is 1.68 cm^2. We set coil 1 to 10 turns, and the area after including the number of turns amounts to 100 cm^2.

Rotation 1: In Fig. 6(a), the 3D orthogonal receiver coils are rotated around the Y-axis. Fig. 7(a) shows a front-facing view of the 3D orthogonal receiver coils with coil 3 set at 5 turns. The area after turns of coil 3 amounts to 8.4 cm^2, about 8.4% of the power transmitted through coil 1 with 10 turns. Based on the effective area of coil 3, we can expect no significant increase in power, as seen in Fig. 7(b). Under the effects of Rotation 1, we see coil 3 with 5 turns contributes to a mere 1.4 to 2.6 dB increase in the total power transmitted compared to the power transmitted in coil 1 with 10 turns alone.

In Fig. 8(a), we increase the number of turns in coil 3 from 5 turns to 15 turns. After the number of turns, the area amounts to 25.2 cm^2, about 25.2% of the power transmitted through coil 1 with 10 turns. Based on the effective area, we see coil 3 contributes between 1.9 dB to 3.4 dB increase in the total power transmitted compared to the power transmitted in coil 1 with 10 turns alone. As expected, we see no power transmission from coil 2, facing the horizontal direction.

Rotation 2: Fig. 6(b) shows the rotational effects of the 3D orthogonal receiver coils around the X-axis. Fig. 9(b) shows increased power transmission from coil 2 at a rotation angle of plus/minus 60°. With coil 2 at 5 turns, the area after turns amounts to 16.55 cm^2 or 16.55% of the power transmitted through coil 1 with 10 turns. Under the effects of Rotation 2, we see coil 2 with 5 turns contributes between 1.9 to 4.3 dB increase in the total power transmitted compared to the power transmitted in coil 1 with 10 turns alone. The increased power transmission of coil 2 at 5 turns compared to coil 3 at 5 turns is due to coil 2 having a larger effective area than coil 3.

In Fig. 10(a), we increase the number of turns of coil 2 from 5 turns to 15 turns. After the number of turns, the area totals 49.7 cm^2 or 49.7% of the power transmitted through coil 1 with 10 turns. Based on the effective area, we see coil 2 contributes between 2.3 dB to 5.4 dB increase in the total power transmitted compared to the power transmitted in coil 1 with 10 turns alone. As expected, we see no power transmission from coil 3, facing the vertical direction.

Rotation 3: Fig. 6(c) shows the 3D orthogonal receiver coils rotated around the Z-axis. Fig. 11 shows no change in power transmission from coils 2 and 3, resulting in no change in total power transmission.

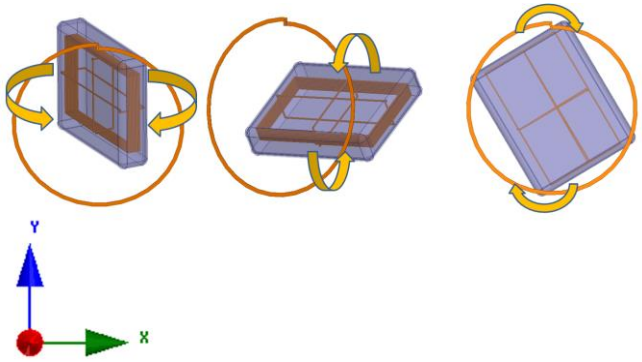

(a) (b) (c)

Fig. 6. Three Rotations around each axis, all at the same angle of -/+ 60°degrees of rotation: **Rotation 1** (a), **Rotation 2** (b), and **Rotation 3** (c).

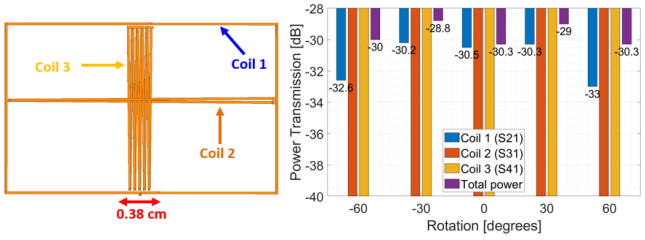

(a) (b)

Fig. 7. Coil 1: 10 turns, Coil 2: 1 turn, Coil 3: 5 turns: (a) Front view of 3D orthogonal coils, (b) Power Transmission as a function of Rotation 1.

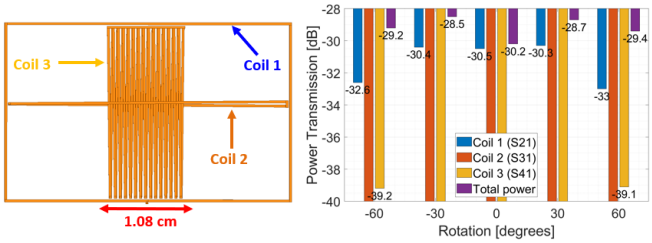

(a) (b)

Fig. 8. Coil 1: 10 turns, Coil 2: 1 turn, Coil 3: 15 turns: (a) Front view of 3D orthogonal coils, (b) Power Transmission as a function of Rotation 1.

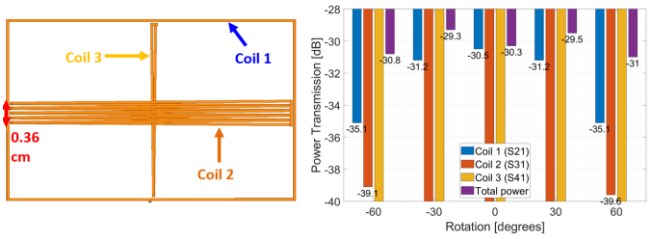

(a) (b)

Fig. 9. Coil 1: 10 turns, Coil 2: 5 turn, Coil 3: 1 turn: (a) Front view of 3D orthogonal coils, (b) Power Transmission as a function of Rotation 2.

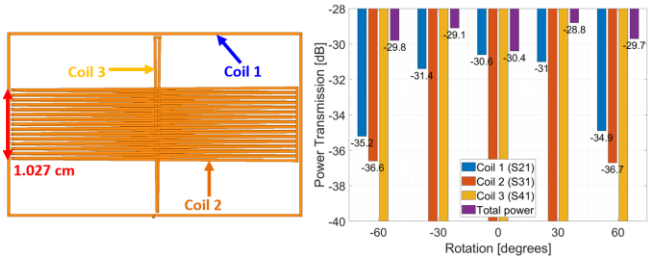

(a) (b)

Fig. 10. Coil 1: 10 turns, Coil 2: 15 turn, Coil 3: 1 turn: (a) Front view of 3D orthogonal coils, (b) Power Transmission as a function of Rotation 2.

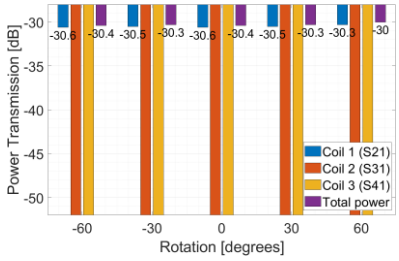

Fig. 11. Power Transmission as a function of Rotation 3.

Lastly, we conducted a parametric study of increasing the number of turns in coils 2 and 3 from 1 to 20. The results showed increases in power transfer efficiency when the height of these coils did not exceed 1/3 to 1/2 of the corresponding dimensions of the implantable unit. Exceeding these dimensions for coils 2 and 3 resulted in interference between coils and reduced power transfer efficiency.

B. Metamaterial Lens

Two metamaterial boards were used in this study. The first is a high-frequency metamaterial lens used at 15 MHz, shown in Fig. 12(a) [6]. The other is a redesigned lens for operating in the lower frequencies often used in commercially available medical units, shown in Fig. 12(b).

At 15 MHz, the inductance value of 3 μH was calculated using the impedance value given in HFSS. Using the inductance value, we calculated the lumped capacitance value using Eqn. (1) set at 35 pF for all four coils of the metamaterial lens. The high-frequency metamaterial lens achieved an S_{21} = -34.2 dB.

This resulted in a 4.8 dB increase in power transmitted with the metamaterial lens.

When testing the original design metamaterial lens at lower frequencies, around 1 MHz, we found that it disrupted the power transmission between the transmitter and the receiver. To achieve lower frequencies, we needed a different metamaterial lens. Lowering in frequency caused us to increase the number of turns of the metamaterial lens coils. While maintaining the original FR4 substrate dimensions, the modified low-frequency design shown in Fig. 12(b) achieves a 5.9 dB increase in power transmitted compared to the WPT system without the metamaterial at 1 MHz.

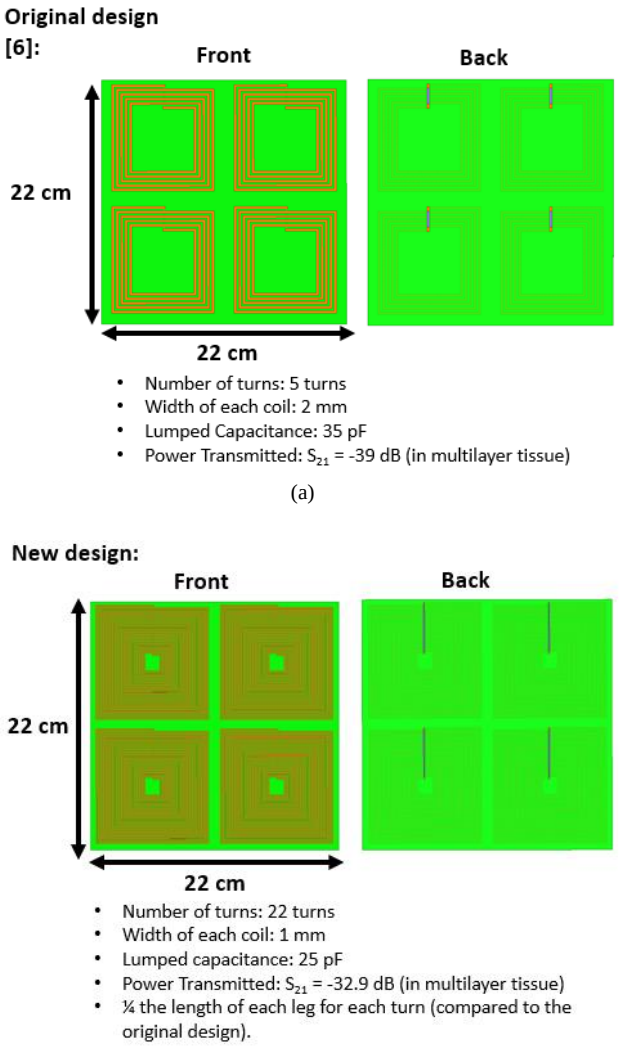

Fig. 12. The metamaterial lens: (a) Original design, (b) New design with an increased number of turns.

Table 1 lists the lumped capacitance values of the new redesigned metamaterial lens tested at lower frequencies. Tuning the new metamaterial lens design at a separation distance of 1 cm from the skin's surface increased power transmission between 3.2 dB to 7.6 dB at a frequency range between 100 kHz and 5 MHz.

TABLE I

LUMPED CAPACITANCE VALUES OF METAMATERIAL BOARD TESTED AT LOWER FREQUENCIES 1 CM SEPARATION DISTANCE AWAY FROM MULTI-LAYER TISSUE.

Frequency (kHz)	Size of metamaterial FR4 substrate (mm)	Inductance (μH)	Capacitance (nF)	Power transmission without metamaterial (dB)	Power transmission with metamaterial (dB)	Increase (dB)
5000	220 x 220	27	**0.04**	-38.8	**-32.5**	**6.3**
1000	220 x 220	25	**1.1**	-38.8	**-32.9**	**5.9**
750	220 x 220	25	**1.97**	-38.8	**-31.2**	**7.6**
500	220 x 220	25	**4.44**	-38.8	**-31.5**	**7.3**
400	220 x 220	25	**6.98**	-38.8	**-32.3**	**6.5**
300	220 x 220	25	**12.4**	-38.8	**-33.3**	**5.5**
200	220 x 220	25	**27.5**	-38.8	**-34.4**	**4.4**
100	220 x 220	25	**108**	-38.8	**-35.6**	**3.2**

Using the new design, we tested the effects of separation distance away from the skin's surface at different frequencies. We tuned the metamaterial lens to the same lumped capacitance value in Table 1 for each given frequency. The separation distance range was from 0.5 cm to 5.5 cm from the skin's surface at a frequency range between 100 kHz and 750 kHz, as shown in Fig. 13. We observed from this figure that the metamaterial surface needs to be within 0.5-2 cm away from the surface of the human body. This is needed to minimize the interaction with the tissues and the possible detuning of the metamaterial lens.

The figure and table show the redesigned metamaterial lens improves power transfer efficiency, presents the capability of tuning the metamaterial lens from 100 kHz to 5 MHz, and achieves a significant increase in power transmission received for all cases.

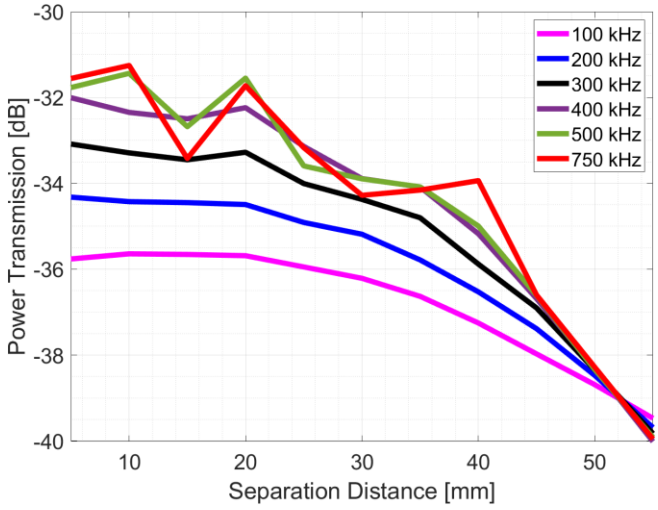

Fig. 13. Separation distances (0.5 cm- 5.5 cm away from skin's surface) at: 100 kHz (pink) with a lumped capacitance value of 108 nF, 200 kHz (blue) with a lumped capacitance value of 27.5 nF, 300 kHz (black) with a lumped capacitance value of 12.4 nF, 400 kHz (purple) with a lumped capacitance value of 6.98 nF, 500 kHz (green) with a lumped capacitance value of 4.44 nF, 750 kHz (red) with a lumped capacitance value of 1.97 nF.

IV. Conclusion

This paper examined avenues for improving the wireless power transmission efficiency to implantable medical devices. Two approaches were studied, implementing three receiving coils in the implantable unit and including a metamaterial lens in a WPT system. Simulations were conducted using 3D, realistic multi-layer cross-section of human body, reported complex permittivity properties as a function of frequency, and High Frequency Structure Simulator (HFSS) used to calculate transmission and reflection coefficient parameters. In summary, the simulation results showed that implementing the 3-coil arrangement in the implantable devices mitigates rotation effects. In some cases, it was observed that the inclusion of three orthogonal coils increased the total power received by the implantable unit. The 3-coil arrangement and associated increase in power transmission efficiency may also enable a lower-powered transmitter coil, thus lowering the risk of tissue absorption within the human body. Additionally, simulation results of a redeveloped metamaterial lens tuned to achieve resonance at lower frequencies improved the power transmission efficiency in the WPT system. We increased the inductance by increasing the number of turns and adjusted the lumped capacitance values for all unit cells on the metamaterial lens. As described, the simulation results showed an increase in power transmission by 3.2 dB to 7.6 dB while meeting set frequencies in commercially available implantable devices ranging between 100 kHz and 5 MHz. Future development may include increasing the number of unit cells on the metamaterial lens for efficiency improvement in misaligned wireless power transfer [11] and validating all results experimentally.

Acknowledgment

This work was supported in part by the U.S. National Science Foundation under Grant 1822213.

References

[1] S. R. Khan, S. K. Pavuluri, G. Cummins, and M. P. Desmulliez, "Wireless power transfer techniques for Implantable Medical Devices: A Review," *Sensors*, vol. 20, no. 12, pp. 10-20, Jun. 2020

[2] Z. Dai, Z. Fang, H. Huang, Y. He, and J. Wang, "Selective Omnidirectional Magnetic Resonant Coupling Wireless Power Transfer With Multiple-Receiver System," *IEEE Access*, vol. 6, pp. 19287–19294, 2018, doi: 10.1109/ACCESS.2018.2809797.

[3] Z. Zhang and B. Zhang, "Angular-Misalignment Insensitive Omnidirectional Wireless Power Transfer," *IEEE Trans. Ind. Electron.*, vol. 67, no. 4, pp. 2755–2764, Apr. 2020, doi: 10.1109/TIE.2019.2908604.

[4] R. Carta, J. Thoné, and R. Puers, "A Wireless Power Supply System for robotic capsular endoscopes," *Sensors and Actuators A: Physical*, vol. 162, no. 2, p. 179, Jan. 2010.

[5] M. Basar, M. Ahmad, J. Cho, and F. Ibrahim, "Application of wireless power transmission systems in wireless capsule endoscopy: An overview," *Sensors*, vol. 14, no. 6, p. 10931, Jun. 2014

[6] D. Shan, H. Wang, K. Cao, and J. Zhang, "Wireless power transfer system with enhanced efficiency by using frequency reconfigurable metamaterial," *Sci Rep*, vol. 12, no. 1, p. 331, Dec. 2022, doi: 10.1038/s41598-021-03570-8.

[7] G. Lipworth *et al.*, "Magnetic Metamaterial Superlens for Increased Range Wireless Power Transfer," *Sci Rep*, vol. 4, no. 1, p. 3642, May 2015, doi: 10.1038/srep03642.

[8] H. Wang, W. Wang, X. Chen, Q. Li, and Z. Zhang, "Analysis and Design of kHz-Metamaterial for Wireless Power Transfer," *IEEE Trans. Magn.*, vol. 56, no. 8, pp. 1–5, Aug. 2020, doi: 10.1109/TMAG.2020.3001360.

[9] "Dielectric Properties » IT'IS Foundation." https://itis.swiss/virtual-population/tissue-properties/database/dielectric-properties/ (accessed Aug. 24, 2022).

[10] B. Wong, S. Clemens, M. F. Iskander, and Z. Yun, "Improvement of Wireless Power Transmission Efficiency to Implantable Devices," in *2022 IEEE International Symposium on Antennas and Propagation and North American Radio Science Meeting*, 2022.

[11] W. Lee and Y.-K. Yoon, "Tunable Metamaterial Slab for Efficiency Improvement in Misaligned Wireless Power Transfer," *IEEE Microw. Wireless Compon. Lett.*, vol. 30, no. 9, pp. 912–915, Sep. 2020, doi: 10.1109/LMWC.2020.3015680.

2022 IEEE International Symposium on Antennas and Propagation and USNC-URSI Radio Science Meeting (AP-S/USNC-URSI) | 978-1-6654-9658-2/22/$31.00 ©2022 IEEE | DOI: 10.1109/AP-S/USNC-URSI47032.2022.9886102

Improvement of Wireless Power Transmission Efficiency to Implantable Devices

B. Wong, S. Clemens, M. F. Iskander, Z. Yun
Hawaii Advanced Wireless Technologies Institute
University of Hawaii at Manoa
Honolulu, USA
blakee@hawaii.edu, scottkc@hawaii.edu, magdy@hawaii.edu, zyun@hawaii.edu

***Abstract*— In this paper we examine the advantages of incorporating three orthogonal coils in the implantable receiving unit to improve the power efficiency under device rotation within the human body. The wireless power transmission system incorporates a realistic multi-layered tissue model and the power transfer process is simulated using High-Frequency Structure Simulator (HFSS) software. The results show that the external and implantable devices can be optimized with improved power transfer efficiency under the effects of rotation within the human body.**

I. Introduction

Large separation distances between transmitting and receiving coils, angular and transpositional misalignment between coils, and tissue losses limit the power transmission performance in Non-Radiative Inductive Coupling (NRIC) wireless power transmission (WPT) systems [1]. We propose to add more receiving coils to collect more power and improve the power transfer efficiency. A 3D design with orthogonal coils used in Wireless Capsule Endoscopy (WCE) power transmission is adopted for receiving coils. They are positioned around a central axis, maximizing the power transmission under rotation effects. When the three orthogonal coils are not perfectly in line with the transmitter coil field lines, the field lines missed by one coil are received by the other two coils [2]. Like NRIC, WCE implantable devices face challenges in power efficiency due to the significant separation distances between the transmitting (Tx) and receiving (Rx) coil, unpredictability in capsules orientation and motion, and the need for compact size of the receiving coil [3]. Our wireless power transmission design increases power received while minimizing interferences among the receiving coils.

II. System Design

An adult male's torso representation comprises a multilayer elliptical cylinder with a width of torso w_{torso} = 280 mm, depth of torso d_{torso} = 360 mm, and a height of torso h_{torso} = 500 mm. The multi-layered cylinders consist of three different biological tissues: skin (external layer of thickness t_s = 3 mm), fat (intermediate layer of thickness t_f = 50 mm), muscle (inner part). The dielectric properties at 40 kHz of the biological tissues are:

Skin: $\varepsilon_r = 1130$, $\mu_r = 1$, $\sigma = 0.000249$ (S/m);
Fat: $\varepsilon_r = 215$, $\mu_r = 1$, $\sigma = 0.0242$ (S/m);
Muscle: $\varepsilon_r = 11000$, $\mu_r = 1$, $\sigma = 0.35$ (S/m);

The titanium case encapsulates the orthogonal Rx coils protecting the surrounding tissues. The dimensions of the titanium case are 43 x 35 x 10 (mm) with a thickness of 0.25 mm. The Rx coils are modelled inside a titanium case with a conductivity of 5.85×10^5 (S/m) which is placed within the abdominal fat layer of the human body model.

The implantation of the single-turn 3D rectangular orthogonal receiver (Rx) coils' dimensions begins with the largest coil facing the transmitting coil represented as coil #1 is l_{rx1} = 40 mm, w_{rx1} = 25 mm. The intermediate coil faced horizontally represents coil #2 is l_{rx2} = 39 mm, w_{rx2} = 8.75 mm. The innermost coil faced vertically represents coil #3 is l_{rx3} = 24 mm, w_{rx3} = 7.5 mm. Each receiving coil has a single turn which is a thin wire with a cross-sectional area of 0.1mm^2.

The transmitter (Tx) coil will be located on the skin surface in front of the subcutaneous Rx coils to reduce the distance between the Tx and Rx. The single turn circular planar Tx coil has a diameter D_{tx} = 52.8 mm. The transmitter coil is slightly larger than the receiving coils to sufficiently tolerate misalignment conditions.

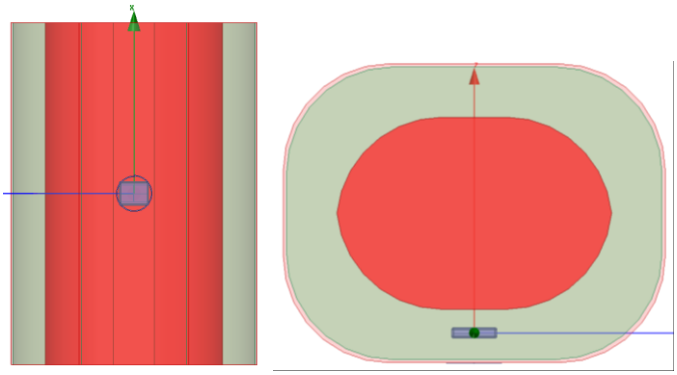

Figure 1 Transmitter and 3D orthogonal receiver coils in the multi-layered tissue model: Side view (left) and Top-down view (right).

III. Results

We examine the performance of the 3D orthogonal receiver coils for three rotations around the central coordinate axis. The power transmission for each coil is recorded, performing a +/-60° rotation around each axis, with steps of 30°. The total power is the sum of the powers received by each of the three Rx coils.

Rotation 1: in Fig. 2 (a), the 3D orthogonal receiver coils are rotated around the X-axis. In Fig. 3 (a), we can see an increase in power transmission for coil 3 at an increase in rotation angle. At angles +/- 60°, coil 3 achieves approximately 80% of the power transmitted for coil 1, around a 9 dB difference between coils, increasing total power transmission by approximately 3 dB compared to having coil 1 alone. Similarly at a rotation angle of +/- 30°, coil 3 achieves approximately 68% of the power transmitted for coil 1, about 16 dB difference between coils. Resulting in a 1.3 dB increase in total power transmission compared to having coil 1 alone. As expected, we see no power transmission from coil 2, facing the horizontal direction.

Rotation 2: Fig. 2 (b) shows the rotational effects of the 3D orthogonal receiver coils around the Y-axis. Fig. 3 (b) shows increased power transmission from coil 3 at a rotation angle of +/- 60°. At angles +/- 60°, coil 2 achieves approximately 92% of the power transmitted for coil 1, around a 3.5 dB difference between coils, increasing the total power transmission by approximately 4.5 dB compared to having coil 1 independently. With a rotation angle of +/- 30°, coil two achieves approximately 74% of the power transmitted for coil one, which averages about a 12.5 dB difference between coils. Resulting in a 2 dB increase in total power transmission compared to having coil 1 alone. As expected, we see no power transmission from coil 3, facing the vertical direction.

Rotation 3: Fig. 2 (c) shows the 3D orthogonal receiver coils around the Z-axis. Fig. 3 (c) shows no change in power transmission from coil 2 and 3 resulting in no change in total power transmission.

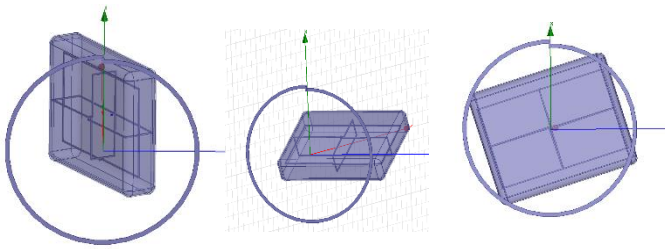

(a) (b) (c)

Figure 2: Three Rotations around each axis, all at the same angle of -60°degrees of rotation: **Rotation 1** (a), **Rotation 2** (b), and **Rotation 3** (c).

IV. Conclusion

The simulation results show that the NRIC wireless power transmission system incorporating 3D orthogonal receiving coils maximizes the power transmission under rotation effects. In the case of **Rotation 2**, the power transmitted by coil 2 achieves approximately 92% of the power transmitted for coil 1, ensuing a 4.5 dB increase in total power transmission compared to having coil 1 alone. The power transmission system also mitigates the power losses caused by misaligned transmitting and receiving coils. Design parameters such as the number of turns for each receiving coil will be examined to maximize power efficiency while minimizing interference between coils. Further improvement of power transfer efficiency using metamaterials to focus powers will be investigated.

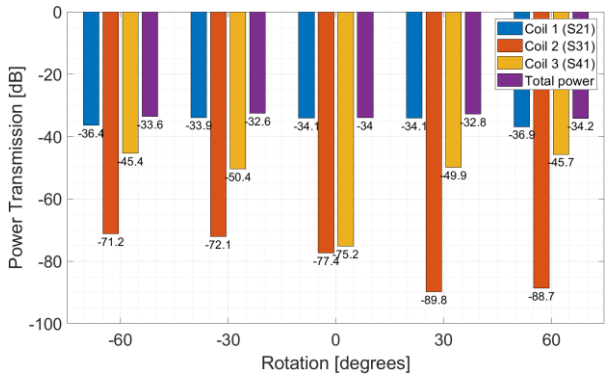

Figure 3 (a) Power Transmission as a function of Rotation 1.

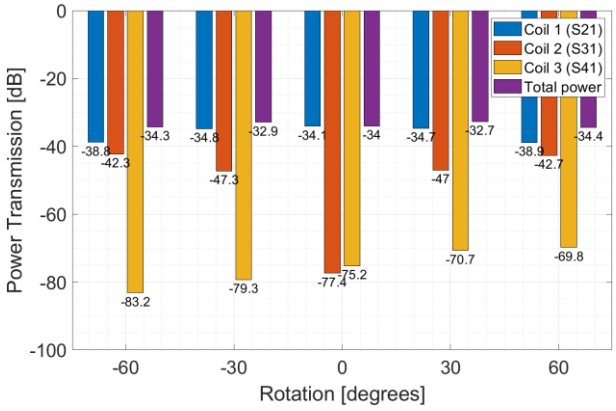

Figure 3 (b) Power Transmission as a function of Rotation 2.

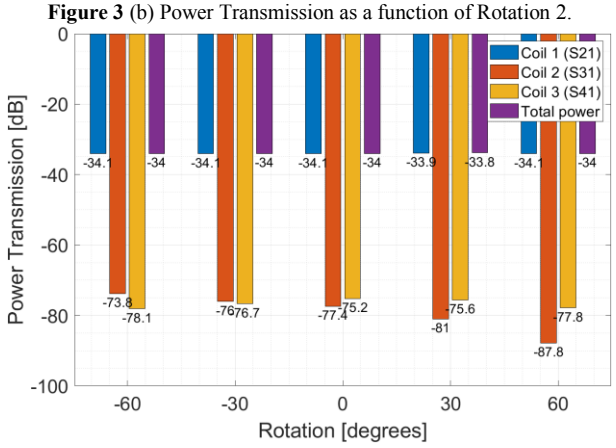

Figure 3 (c) Power transmission as a function of Rotation 3.

References

[1] S. R. Khan, S. K. Pavuluri, G. Cummins, and M. P. Desmulliez, "Wireless power transfer techniques for Implantable Medical Devices: A Review," *Sensors*, vol. 20, no. 12, pp. 10-20, Jun. 2020.

[2] R. Carta, J. Thoné, and R. Puers, "A Wireless Power Supply System for robotic capsular endoscopes," *Sensors and Actuators A: Physical*, vol. 162, no. 2, p. 179, Jan. 2010.

[3] M. Basar, M. Ahmad, J. Cho, and F. Ibrahim, "Application of wireless power transmission systems in wireless capsule endoscopy: An overview," *Sensors*, vol. 14, no. 6, p. 10931, Jun. 2014.